

# Spontaneous decay of an excited atom in an absorbing dielectric

S. Scheel, L. Knöll, and D.-G. Welsch

*Theoretisch-Physikalisches Institut, Friedrich-Schiller-Universität Jena, Max-Wien-Platz 1, 07743*

*Jena, Germany*

(June 13, 2018)

## Abstract

Starting from the quantized version of Maxwell's equations for the electromagnetic field in an arbitrary linear Kramers-Kronig dielectric, spontaneous decay of the excited state of a two-level atom embedded in a dispersive and absorbing medium is studied and the decay rate is calculated. The calculations are performed for both the (Clausius-Mosotti) virtual cavity model and the (Glauber-Lewenstein) real cavity model. It is shown that owing to nonradiative decay associated with absorption the rate of spontaneous decay sensitively depends on the cavity radius when the atomic transition frequency approaches an absorption band of the medium. Only when the effect of absorption is fully disregarded, then the familiar local-field correction factors are recovered.

42.50.-p,42.50.Ct,42.50.Lc

Typeset using REVTeX

## I. INTRODUCTION

Spontaneous emission is a prime example of the action of vacuum fluctuations on physically measurable processes. Since the early work of Einstein [1] spontaneous emission has been a major ingredient in the understanding of the effects of what one calls the vacuum in quantum field theory. The radiation properties of an excited atom located in free space have been a subject of many studies (for a comprehensive list of original articles, see, e.g., [2]). In particular, the rate of spontaneous emission in free space (half the Einstein coefficient) is given by

$$\Gamma_{\text{SE}} = \Gamma_0 \equiv \frac{\omega_A^3 \mu^2}{3\pi \hbar \epsilon_0 c^3}, \quad (1)$$

where  $\omega_A$  is the transition frequency of the atom and  $\mu$  is the dipole matrix element of the transition. The question has been arisen of how a surrounding medium modifies that decay. Simple arguments based on the change of the mode density suggest that the spontaneous emission rate inside a non-absorbing dielectric should be modified according to [3]

$$\Gamma_{\text{SE}} = n\Gamma_0, \quad (2)$$

where  $n$  is the real refractive index of the medium. In Eq. (2) it is assumed that the local field the atom interacts with is identical with the electromagnetic field in the continuous medium. Since in reality the atom is in a small region of free space, the local field felt by the atom is different from the field in the continuous medium [4], and the decay rate may be expected to be modified to

$$\Gamma_{\text{SE}} = n\xi\Gamma_0, \quad (3)$$

where  $\xi$  is the local-field correction factor. Different models have been used to calculate it. In the (Clausius-Mosotti) virtual cavity model it is given by [5]

$$\xi_{\text{CM}} = \left( \frac{n^2 + 2}{3} \right)^2, \quad (4)$$

whereas the (Glauber-Lewenstein) real cavity model leads to [6]

$$\xi_{\text{GL}} = \left( \frac{3n^2}{2n^2 + 1} \right)^2. \quad (5)$$

Recently, experiments have been reported [7,8] from which the real-cavity model may be favored.

As already mentioned, in Eqs. (2) – (5) it is assumed that the refractive index of the medium, which may vary with frequency [i.e.,  $n \rightarrow n(\omega_A)$  in Eqs. (1.2) – (1.5)], is real. However, in reality the refractive index must be a complex function of frequency,

$$n(\omega) = \eta(\omega) + i\kappa(\omega). \quad (6)$$

It is well known that causality requires the permittivity of the medium,  $\epsilon(\omega) = n^2(\omega)$ , to be a complex function of frequency whose real part (responsible for dispersion) and imaginary part (responsible for absorption) are related to each other by the Kramers-Kronig relation. Only when the atomic transition frequency  $\omega_A$  is sufficiently far from a medium resonance, so that absorption may be disregarded, the imaginary part of the refractive index (at the atomic transition frequency) may be neglected:  $n(\omega_A) \approx \eta(\omega_A)$ .

Describing the (undisturbed, continuous) medium in terms of a complex permittivity, in [9,10] it is argued that Eqs. (3) – (5) can be extended to the spontaneous emission of an atom embedded in a lossy dielectric as

$$\Gamma_{\text{SE}} = \eta(\omega_A)\xi(\omega_A)\Gamma_0, \quad (7)$$

where the local-field correction factors (4) and (5) are now regarded as being squares of absolute values,

$$\xi_{\text{CM}}(\omega_A) = \left| \frac{n^2(\omega_A) + 2}{3} \right|^2, \quad (8)$$

$$\xi_{\text{GL}}(\omega_A) = \left| \frac{3n^2(\omega_A)}{2n^2(\omega_A) + 1} \right|^2. \quad (9)$$

Further, in [10] the total decay rate is decomposed as

$$\Gamma = \Gamma^\perp + \Gamma^\parallel, \quad (10)$$

where the rates  $\Gamma^\perp$  and  $\Gamma^\parallel$ , respectively, are related to the transverse and longitudinal electromagnetic fields in the medium. The rate  $\Gamma^\perp$  is identified with the cavity-radius-independent rate  $\Gamma_{\text{SE}}$  given by Eq. (7), and it is argued that the rate  $\Gamma^\parallel$ , which depends on the cavity radius  $R$  as  $\Gamma^\parallel \sim R^{-3}$ , is responsible for nonradiative decay via energy transfer between the atom and the surrounding (absorbing) dielectric.

From the study of resonant energy transfer between two guest molecules in a perfect lattice of absorbing molecules [11], in [12] it is argued that (within the approximations made) the rate of spontaneous emission is given by Eq. (7) together with Eq. (8), i.e., with the local-field correction factor that corresponds to the virtual-cavity model. However, the total decay rate is purely transverse; i.e., it results only from the transverse part of the electromagnetic field in the medium,

$$\Gamma = \Gamma^\perp = \Gamma^{(1)} + \Gamma^{(2)}. \quad (11)$$

It consists of an  $R$ -independent far-field term  $\Gamma^{(1)}$ , which has the form of Eq. (7) [together with Eq. (8)] and is interpreted as the spontaneous emission rate, and a  $R$ -dependent term  $\Gamma^{(2)}$ , which in the near-field zone is proportional to  $R^{-3}$  and describes nonradiative energy transfer.

Recently it has been shown [13] that the decay rates suggested in [9,10] for the virtual-cavity model are wrong in general, because the quantum vacuum in the presence of a dispersive and absorbing dielectric is not introduced correctly. The fluctuating part of the polarization field is not fully included in the local field coupled to the atom and therefore effects such as nonradiative energy transfer from the guest atom to the medium via virtual photon exchange (i.e., transverse-field-assisted energy transfer) are omitted. It is just the contribution to the local field of the fluctuating part of the polarization which gives rise to the relevant terms  $\sim R^{-3}$  and  $\sim R^{-1}$  in the transverse decay rate of an excited atom surrounded by an absorbing medium [13]. It is worth noting that the results have been confirmed within a microscopic approach to the problem more recently [14].

In the virtual-cavity model, the electromagnetic field inside the cavity, i.e., the local

field, is modified by the presence of the cavity, but the modification of the field outside the cavity is disregarded. Hence the local field introduced in this way is not exactly the field that couples to the atom in reality. On the contrary, in the real-cavity model the mutual modification of the fields outside and inside the cavity are taken into account in a consistent way; i.e., the atom interacts with a field that exactly satisfies both Maxwell's equations and the fundamental commutation rules of quantum electrodynamics. It may be therefore expected that the real cavity model is more suited for describing the spontaneous decay than the virtual cavity model. In particular, the Power-Zienau-Woolley transformation (see, e.g., [15]) suggests that (in dipole approximation) only the transverse electromagnetic field contributes to the decay rate via radiative decay *and* nonradiative decay associated with virtual photon exchange, the latter being typical for an absorbing medium.

In this article we consider, within the frame of rigorous quantization of the electromagnetic field in an arbitrary linear Kramers-Kronig consistent dielectric [16–18], the spontaneous decay of an excited atom embedded in an absorbing dielectric, applying the real-cavity concept. We find that the rate formulas suggested in [10] for the real-cavity model are essentially wrong. At first, only the transverse electromagnetic field contributes to the decay rate, i.e.,  $\Gamma^{\parallel} \equiv 0$ , which contradicts [10]. At second, the (purely transverse) rate not only contains an  $R$ -independent term but also terms proportional to  $R^{-1}$  and  $R^{-3}$  which are closely related to nonradiative decay – a result which also contradicts [10]. As expected, nonradiative decay is only observed for an absorbing medium. It is worth noting that when the atomic transition frequency is sufficiently far from an absorption band of the medium, so that absorption may be neglected, our result exactly agrees with that derived in [6] for a non-absorbing medium.

The paper is organized as follows. After introducing the quantization scheme, in Sect. II the problem of spontaneous decay of an excited atom in an absorbing medium is considered. In Sect. III the results for decay rate with the virtual cavity model are outlined, and Sect. IV presents a detailed analysis of the decay rate with the real cavity model. The results are discussed in Sect. V. Lengthy calculations are given in the Appendix.

## II. BASIC EQUATIONS

Our analysis of the spontaneous decay of an excited atom embedded in an absorbing medium is based on the scheme for quantization of the electromagnetic field in linear Kramers-Kronig dielectrics developed in [16–18]. We start with the phenomenological Maxwell's equations in the (temporal) Fourier space, without external sources,

$$\nabla \cdot \hat{\mathbf{B}}(\mathbf{r}, \omega) = 0, \quad (12)$$

$$\nabla \cdot [\epsilon_0 \epsilon(\mathbf{r}, \omega) \hat{\mathbf{E}}(\mathbf{r}, \omega)] = \hat{\rho}(\mathbf{r}, \omega), \quad (13)$$

$$\nabla \times \hat{\mathbf{E}}(\mathbf{r}, \omega) = i\omega \hat{\mathbf{B}}(\mathbf{r}, \omega), \quad (14)$$

$$\nabla \times \hat{\mathbf{B}}(\mathbf{r}, \omega) = -i\frac{\omega}{c^2} \epsilon(\mathbf{r}, \omega) \hat{\mathbf{E}}(\mathbf{r}, \omega) + \mu_0 \hat{\mathbf{j}}(\mathbf{r}, \omega), \quad (15)$$

where  $\epsilon(\mathbf{r}, \omega) = \epsilon_R(\mathbf{r}, \omega) + i\epsilon_I(\mathbf{r}, \omega)$  is the (spatially varying) permittivity satisfying the Kramers-Kronig relations. When there are no external charges and currents, then  $\hat{\rho}(\mathbf{r}, \omega)$  and  $\hat{\mathbf{j}}(\mathbf{r}, \omega)$ , respectively, are the operator noise charge and current densities that are associated with absorption according to the dissipation-fluctuation theorem. They satisfy the equation of continuity,

$$\nabla \cdot \hat{\mathbf{j}}(\mathbf{r}, \omega) = i\omega \hat{\rho}(\mathbf{r}, \omega), \quad (16)$$

and they are related to the noise polarization  $\hat{\mathbf{P}}^N(\mathbf{r}, \omega)$  as

$$\hat{\mathbf{j}}(\mathbf{r}, \omega) = -i\omega \hat{\mathbf{P}}^N(\mathbf{r}, \omega), \quad (17)$$

$$\hat{\rho}(\mathbf{r}, \omega) = -\nabla \cdot \hat{\mathbf{P}}^N(\mathbf{r}, \omega). \quad (18)$$

Let  $\hat{\mathbf{f}}(\mathbf{r}, \omega)$  be an infinite set of bosonic field operators which may be viewed as being collective excitations of the electromagnetic field, the medium polarization, and the reservoir. All operators in the theory can then be expressed in terms of these basic field operators using the relation

$$\hat{\underline{\mathbf{j}}}(\mathbf{r}, \omega) = \omega \sqrt{\frac{\hbar \epsilon_0}{\pi}} \epsilon_I(\mathbf{r}, \omega) \hat{\mathbf{f}}(\mathbf{r}, \omega). \quad (19)$$

In particular, from Maxwell's equations the electric field (in Fourier space) is given by a convolution with the classical dyadic Green function,

$$\hat{\underline{E}}_k(\mathbf{r}, \omega) = i\mu_0 \int d^3\mathbf{r}' \omega G_{kk'}(\mathbf{r}, \mathbf{r}', \omega) \hat{\underline{j}}_{k'}(\mathbf{r}', \omega), \quad (20)$$

where  $G_{kk'}(\mathbf{r}, \mathbf{r}', \omega)$  satisfies the partial differential equation

$$\left[ \partial_i^r \partial_k^r - \delta_{ik} \left( \Delta^r + \frac{\omega^2}{c^2} \epsilon(\mathbf{r}, \omega) \right) \right] G_{kk'}(\mathbf{r}, \mathbf{r}', \omega) = \delta_{ik'} \delta(\mathbf{r} - \mathbf{r}'). \quad (21)$$

Integration with respect to  $\omega$  then yields the operator of the electric field as

$$\hat{\mathbf{E}}(\mathbf{r}) = \hat{\mathbf{E}}^{(+)}(\mathbf{r}) + \hat{\mathbf{E}}^{(-)}(\mathbf{r}), \quad \hat{\mathbf{E}}^{(-)}(\mathbf{r}) = [\hat{\mathbf{E}}^{(+)}(\mathbf{r})]^\dagger, \quad (22)$$

$$\hat{E}_k^{(+)}(\mathbf{r}) = \int_0^\infty d\omega \hat{\underline{E}}_k(\mathbf{r}, \omega) = i\mu_0 \int_0^\infty d\omega \int d^3\mathbf{r}' \omega G_{kk'}(\mathbf{r}, \mathbf{r}', \omega) \hat{\underline{j}}_{k'}(\mathbf{r}', \omega). \quad (23)$$

Substituting in Eq. (23) for the current density the expression given in Eq. (19) yields the electric field in terms of the bosonic basic fields. It can be proven [18] that the quantization scheme is fully consistent with QED for arbitrary linear dielectrics, i.e.,

$$\epsilon_0 [\hat{E}_k(\mathbf{r}), \hat{B}_l(\mathbf{r}')] = -i\hbar \epsilon_{klm} \partial_m^r \delta(\mathbf{r} - \mathbf{r}'), \quad (24)$$

$$[\hat{E}_k(\mathbf{r}), \hat{E}_l(\mathbf{r}')] = [\hat{B}_k(\mathbf{r}), \hat{B}_l(\mathbf{r}')] = 0. \quad (25)$$

The electric and magnetic fields can be of course expressed in terms of vector ( $\hat{\mathbf{A}}$ ) and scalar ( $\hat{\varphi}$ ) potentials. In what follows we will set the scalar potential equal to zero. This gauge condition implies that both the transverse and the longitudinal electric fields are obtained from the vector potential

$$\hat{\mathbf{A}}(\mathbf{r}) = \hat{\mathbf{A}}^{(+)}(\mathbf{r}) + \hat{\mathbf{A}}^{(-)}(\mathbf{r}), \quad (26)$$

$$\hat{A}_k^{(+)}(\mathbf{r}) = \mu_0 \int_0^\infty d\omega \int d^3\mathbf{r}' G_{kk'}(\mathbf{r}, \mathbf{r}', \omega) \hat{\underline{j}}_{k'}(\mathbf{r}', \omega). \quad (27)$$

Let us now consider the case when an external (two-level) atomic system at position  $\mathbf{r}_A$  is present. Treating the interaction of such a guest atom with the electromagnetic field in dipole and rotating wave approximations, the Hamiltonian of the total system can be given by

$$\hat{H} = \int d^3\mathbf{r} \int_0^\infty d\omega \hbar\omega \hat{\mathbf{f}}^\dagger(\mathbf{r}, \omega) \hat{\mathbf{f}}(\mathbf{r}, \omega) + \sum_{\alpha=1}^2 \hbar\omega_\alpha \hat{A}_{\alpha\alpha} - [i\omega_{21} \hat{A}_{21} \hat{\mathbf{A}}^{(+)}(\mathbf{r}_A) \cdot \mathbf{d}_{21} + \text{H.c.}] \quad (28)$$

Here the atomic operators  $\hat{A}_{\alpha\alpha'} = |\alpha\rangle\langle\alpha'|$  are introduced, with  $|\alpha\rangle$  being the energy eigenstates of the guest atom ( $\alpha = 1, 2$ ). The energies of the two states are  $\hbar\omega_1$  and  $\hbar\omega_2$  ( $\hbar\omega_2 > \hbar\omega_1$ ), and  $\omega_{21} = \omega_2 - \omega_1$  and  $\mathbf{d}_{21}$ , respectively, are the atomic transition frequency and dipole moment. Note that in the interaction term in Eq. (28) the  $\hat{\mathbf{A}}^2$  term and the counter-rotating terms have been dropped.

In the Heisenberg picture the equations of motion then read as, on recalling Eqs. (19) and (27),

$$\dot{\hat{A}}_{22} = -\frac{\omega_{21}}{\hbar} \hat{A}_{21} \hat{\mathbf{A}}^{(+)}(\mathbf{r}_A) \cdot \mathbf{d}_{21} + \text{H.c.}, \quad (29)$$

$$\dot{\hat{A}}_{11} = -\dot{\hat{A}}_{22}, \quad (30)$$

$$\dot{\hat{A}}_{21} = i\omega_{21} \hat{A}_{21} + \frac{\omega_{21}}{\hbar} \hat{\mathbf{A}}^{(-)}(\mathbf{r}_A) \cdot \mathbf{d}_{21} (\hat{A}_{22} - \hat{A}_{11}), \quad (31)$$

$$\dot{\hat{f}}_i(\mathbf{r}, \omega) = -i\omega \hat{f}_i(\mathbf{r}, \omega) + \frac{\omega_{21}\omega}{c^2} \sqrt{\frac{\epsilon_I(\mathbf{r}, \omega)}{\hbar\pi\epsilon_0}} (d_{21})_k G_{ki}^*(\mathbf{r}_A, \mathbf{r}, \omega) \hat{A}_{12}. \quad (32)$$

Substituting in the vector potential in Eqs. (29) – (31) for  $\hat{f}_i(\mathbf{r}, \omega, t)$  the formal solution of Eq. (32), i.e.,

$$\hat{A}_i^{(+)}(\mathbf{r}, t) = \hat{A}_{\text{free } i}^{(+)}(\mathbf{r}, t) + \frac{\omega_{21}}{\pi\epsilon_0 c^2} (d_{21})_k \int_0^\infty d\omega \left[ \text{Im } G_{ik}(\mathbf{r}, \mathbf{r}_A, \omega) \int_{t'}^t d\tau e^{-i\omega(t-\tau)} \hat{A}_{12}(\tau) \right], \quad (33)$$

a system of integro-differential equations for the atomic quantities is obtained. [Note that Eq. (A3) has been used for deriving Eq. (33).] At this stage a Markov approximation can be introduced, and the integro-differential equations reduce to Langevin-type differential equations (Appendix A)

$$\dot{\hat{A}}_{22} = -\Gamma \hat{A}_{22} - \left[ \hat{A}_{21} \frac{\omega_{21}}{\hbar} \hat{\mathbf{A}}_{\text{free}}^{(+)}(\mathbf{r}_A, t) \cdot \mathbf{d}_{21} + \text{H.c.} \right], \quad (34)$$

$$\dot{\hat{A}}_{11} = -\dot{\hat{A}}_{22}, \quad (35)$$

$$\dot{\hat{A}}_{21} = \left[ i(\omega_{21} - \delta\omega) - \frac{1}{2}\Gamma \right] \hat{A}_{21} + \frac{\omega_{21}}{\hbar} \hat{\mathbf{A}}_{\text{free}}^{(-)}(\mathbf{r}_A, t) \cdot \mathbf{d}_{21} (\hat{A}_{22} - \hat{A}_{11}), \quad (36)$$

where  $\Gamma$  is the rate of spontaneous decay of the excited state of the guest atom,

$$\Gamma = \frac{2\omega_A^2 \mu_k \mu_{k'}}{\hbar \epsilon_0 c^2} \text{Im} G_{kk'}(\mathbf{r}_A, \mathbf{r}_A, \omega_A) \quad (37)$$

$[\mu_k \equiv (d_{21})_k, \omega_A \equiv \omega_{21}]$ , and  $\delta\omega$  is the (contribution of the dielectric to the) Lamb shift [see Eq. (A6)]. Note that  $\hat{\mathbf{A}}_{\text{free}}^{(\pm)}(\mathbf{r}, t)$  evolves freely. From Eq. (20) together with Eqs. (19) and (A3) it can be proved that the quantization scheme exactly yields, in agreement with the dissipation-fluctuation theorem, the relation [19]

$$\text{Im} G_{kk'}(\mathbf{r}, \mathbf{r}', \omega') \delta(\omega - \omega') = \frac{\pi \epsilon_0 c^2}{\hbar \omega^2} \langle 0 | [\hat{\underline{E}}_k(\mathbf{r}, \omega), \hat{\underline{E}}_{k'}^\dagger(\mathbf{r}', \omega')] | 0 \rangle. \quad (38)$$

As long as the Markov approximation applies, the spontaneous decay can be described in terms of the rate (37), the rate formula being valid for arbitrary dielectrics and geometries. Especially, for an atom in vacuum we have

$$\text{Im} G_{kk'}(\mathbf{r}_A, \mathbf{r}_A, \omega_A) = \frac{\omega_A}{6\pi c} \delta_{kk'} \quad (39)$$

[see Eqs. (B1) – (B5) for  $\epsilon = 1$ ], which leads to the well-known result (1),

$$\Gamma = \Gamma_0 = \frac{\omega_A^3 \mu^2}{3\pi \hbar \epsilon_0 c^3}. \quad (40)$$

A guest atom in a dielectric is situated in a small free-space region and is surrounded by medium atoms. Frequently a cavity model is used for describing the situation. An atom in an empty cavity in an otherwise continuous medium is considered and it is assumed that the linear dimensions of the cavity are much less than the atomic transition wavelength. In particular, for isotropic systems a spherical cavity of radius  $R$  may be considered. With regard to Eq. (37), the “only” problem that remains is the calculation of (the imaginary part of) the classical Green tensor for a dielectric medium of given permittivity which is disturbed by a small free-space inhomogeneity.

### III. VIRTUAL CAVITY MODEL

In the virtual cavity model it is assumed that the field outside the sphere is not modified by the small region of free space inside the sphere, and the (local) electric field  $\underline{\mathbf{E}}'(\mathbf{r}, \omega)$  inside the sphere is given by [20]

$$\underline{\hat{\mathbf{E}}}'(\mathbf{r}, \omega) = \underline{\hat{\mathbf{E}}}(\mathbf{r}, \omega) + \frac{1}{3\epsilon_0} \underline{\hat{\mathbf{P}}}(\mathbf{r}, \omega), \quad (41)$$

where  $\underline{\mathbf{E}}(\mathbf{r}, \omega)$  and  $\underline{\mathbf{P}}(\mathbf{r}, \omega)$ , respectively, are the electric and polarization fields in the unperturbed continuous medium. From Maxwell's equations (13) and (15) together with Eqs. (16) – (19) it is seen that

$$\underline{\hat{\mathbf{P}}}(\mathbf{r}, \omega) = \epsilon_0 [\epsilon(\mathbf{r}, \omega) - 1] \underline{\hat{\mathbf{E}}}(\mathbf{r}, \omega) + \underline{\hat{\mathbf{P}}}^N(\mathbf{r}, \omega), \quad (42)$$

where

$$\underline{\hat{\mathbf{P}}}^N(\mathbf{r}, \omega) = i \sqrt{\frac{\hbar \epsilon_0}{\pi}} \epsilon_I(\mathbf{r}, \omega) \hat{\mathbf{f}}(\mathbf{r}, \omega) \quad (43)$$

is the noise polarization associated with absorption. For classical optical fields at room temperatures the noise polarization weakly contributes to the polarization and the local field, and therefore it may be neglected. Obviously, for quantum fields and especially for the quantum vacuum, whose coupling to the guest atom gives rise to the spontaneous decay, the noise polarization must not be omitted, because it is nothing other but a part of the quantum vacuum. Combining Eqs. (41) and (42) yields the local-field operator

$$\underline{\hat{\mathbf{E}}}'(\mathbf{r}, \omega) = \frac{1}{3} [\epsilon(\mathbf{r}, \omega) + 2] \underline{\hat{\mathbf{E}}}(\mathbf{r}, \omega) + \frac{1}{3\epsilon_0} \underline{\hat{\mathbf{P}}}^N(\mathbf{r}, \omega). \quad (44)$$

It can be shown that the local electromagnetic field satisfies the equal-time commutation relations [13]

$$\epsilon_0 [\hat{E}'_k(\mathbf{r}), \hat{B}'_l(\mathbf{r}')] = -i\hbar \epsilon_{klm} \partial_m^r \delta(\mathbf{r} - \mathbf{r}') \left\{ 1 + \frac{1}{9} [\epsilon(\mathbf{r}, 0) - 1] \right\}, \quad (45)$$

$$[\hat{E}'_k(\mathbf{r}), \hat{E}'_l(\mathbf{r}')] = [\hat{B}'_k(\mathbf{r}), \hat{B}'_l(\mathbf{r}')] = 0, \quad (46)$$

Comparing with the correct commutation relations, we see that the virtual cavity model may be regarded as being consistent with QED (over the whole frequency domain), provided that

$$\epsilon(\mathbf{r}, 0) \ll 10; \quad (47)$$

i.e., the value of the static permittivity must not be too large.

Now we can turn to the calculation of the spontaneous decay rate, Eq. (37). Recalling Eq. (38), we may write

$$\text{Im } G_{kk'}(\mathbf{r}, \mathbf{r}', \omega_A) \delta(\omega - \omega_A) = \frac{\pi \epsilon_0 c^2}{\hbar \omega^2} \langle 0 | [\hat{\underline{E}}'_k(\mathbf{r}, \omega), \hat{\underline{E}}_{k'}^\dagger(\mathbf{r}', \omega_A)] | 0 \rangle \quad (48)$$

with  $|\mathbf{r} - \mathbf{r}_A|, |\mathbf{r}' - \mathbf{r}_A| < R$  and  $\hat{\underline{E}}'$  from Eq. (44). Since  $\hat{\underline{E}}$  in Eq. (44) is determined by Eq. (20) with the Green tensor for the field in the undisturbed continuous medium, knowledge of the imaginary part of that Green tensor is sufficient to calculate the decay rate. However, for  $\mathbf{r}, \mathbf{r}' \rightarrow \mathbf{r}_A$  a singular contribution to the rate is observed, which reflects the fact that the description of the dielectric as a continuous medium contradicts a precise determination of the position of the guest atom. The problem might be overcome by regularization, e.g., by averaging Eq. (48) over the sphere. Combining Eqs. (37) and (48) and using Eq. (44) [together with Eqs. (19), (20), and (43)] yields [13]

$$\begin{aligned} \Gamma_{\text{CM}} = & \frac{2\omega_A^2 \mu_k \mu_{k'}}{\hbar \epsilon_0 c^2} \left| \frac{\epsilon(\omega_A) + 2}{3} \right|^2 \text{Im } \overline{G_{kk'}^{\text{M}}(\mathbf{r}, \mathbf{r}', \omega)} \\ & + \frac{4\omega_A^2}{3\hbar \epsilon_0 c^2} \epsilon_I(\omega_A) \mu_k \mu_{k'} \text{Re} \left[ \frac{\epsilon(\omega_A) + 2}{3} \overline{G_{kk'}^{\text{M}}(\mathbf{r}, \mathbf{r}', \omega_A)} \right] + \frac{2}{9\hbar \epsilon_0} \epsilon_I(\omega_A) \mu_k \mu_{k'} \overline{\delta_{kk'} \delta(\mathbf{r} - \mathbf{r}')} \quad (49) \end{aligned}$$

(the bar introduces averaging over the sphere), where  $G_{kk'}^{\text{M}}(\mathbf{r}, \mathbf{r}', \omega)$  is the Green tensor of the mean field in the undisturbed medium, and  $\epsilon(\omega_A) \equiv \epsilon(\mathbf{r}_A, \omega_A)$ . Note that the permittivity can be assumed to be constant over the small sphere. The first term in Eq. (49) corresponds to the result obtained in [9,10], without taking account of the contribution of the noise polarization to the quantum vacuum. The noise polarization gives rise to the second term and the third term in Eq. (49) – terms that are proportional to  $\epsilon_I(\omega_A)$  and typically observed for absorbing media.

When the position of the guest atom in the medium is sufficiently far from inhomogeneities (such as the surface of the dielectric body) the Green tensor  $G_{kk'}^M(\mathbf{r}, \mathbf{r}', \omega)$  in Eq. (49) may be identified with that for bulk material as given in Appendix B. Inserting for  $G_{kk'}^M(\mathbf{r}, \mathbf{r}', \omega_A)$  in Eq. (49) the result of Eqs. (B1), (B2), and (B5) and averaging with respect to  $\mathbf{r}$  and  $\mathbf{r}'$  separately over a sphere, on assuming equidistribution, we derive [21]

$$\Gamma_{\text{CM}} = \Gamma_{\text{CM}}^{\parallel} + \Gamma_{\text{CM}}^{\perp}, \quad (50)$$

where  $\Gamma_{\text{CM}}^{\parallel}$  and  $\Gamma_{\text{CM}}^{\perp}$ , respectively, are related to the longitudinal and transverse parts of the Green tensor,

$$\Gamma_{\text{CM}}^{\parallel} = \Gamma_0 \frac{4\epsilon_I(\omega_A)}{27|\epsilon(\omega_A)|^2} \left( \frac{c}{\omega_A R} \right)^3, \quad (51)$$

$$\begin{aligned} \Gamma_{\text{CM}}^{\perp} = \Gamma_0 \left\{ \eta(\omega_A) \left[ \left| \frac{\epsilon(\omega_A) + 2}{3} \right|^2 - \frac{2\epsilon_I^2(\omega_A)}{9} \right] \right. \\ \left. + \epsilon_I(\omega_A) [\epsilon_R(\omega_A) + 2] \left[ \frac{8}{15} \left( \frac{c}{\omega_A R} \right) - \frac{2}{9} \kappa(\omega_A) \right] + \frac{25\epsilon_I(\omega_A)}{54} \left( \frac{c}{\omega_A R} \right)^3 \right\} + \mathcal{O}(R) \quad (52) \end{aligned}$$

( $|R\sqrt{\epsilon(\omega_A)}\omega_A/c| \ll 1$ ), with  $\Gamma_0$  being the free-space spontaneous emission rate defined in Eq. (1). From inspection of Eqs. (50) – (52) it is seen that, when absorption can be disregarded, i.e.,  $\epsilon_I(\omega_A) \approx 0$  and hence  $\epsilon(\omega_A) \approx \epsilon_R(\omega_A)$ ,  $n(\omega_A) \approx \sqrt{\epsilon_R(\omega_A)}$ , then  $\Gamma_{\text{CM}} \approx \Gamma_{\text{CM}}^{\perp}$  reduces to  $\Gamma_{\text{SE}}$  given in Eq. (3) with the local-field correction factor (4). It is further seen that for absorbing media the rate  $\Gamma_{\text{CM}}^{\perp}$  becomes quite different from that given in Eq. (7) with the local-field correction factor (8), because of the effect of the noise polarization. For more details, the reader is referred to [13]. Most recently, a more microscopic derivation of the decay rate has yielded, apart from regularization factors, the same results [14].

It is worth noting that the  $R$ -dependent terms in Eq. (52) solely result from the noise polarization. In particular, the term  $\sim R^{-3}$  may be regarded as describing nonradiative decay via dipole-dipole energy transfer from the guest atom to the surrounding medium. From Eqs. (50) – (52) it is seen that the terms  $\sim R^{-3}$  can be combined to obtain an overall rate for the nonradiative dipole-dipole energy transfer. Obviously, the decomposition of  $\Gamma_{\text{CM}}$

in  $\Gamma_{\text{CM}}^\perp$  and  $\Gamma_{\text{CM}}^\parallel$  has nothing to do with a decomposition in radiative and nonradiative decay channels in general.

It should be pointed out that the averages in Eq. (49), which correspond to regularization at  $\mathbf{r} \rightarrow \mathbf{r}'$ , can be taken in different ways. In other words, the  $R$ -dependent terms in Eqs. (51) and (52) are determined only up to some regularization factors. Hence, not only the the cavity radius  $R$  but also the scaling factors of the absorption-assisted  $\sim R^{-1}$  and  $\sim R^{-3}$  terms are undetermined in the model.

#### IV. REAL CAVITY MODEL

In the real cavity model the exact Green tensor for the system disturbed by a small free-space inhomogeneity is inserted in the rate formula (37). In other words, the electromagnetic field inside and outside the cavity exactly solves Maxwell's equations (12) – (15) together with the standard boundary conditions at the surface of the cavity. In contrast to the virtual cavity approach, in the real cavity approach the field inside the cavity exactly satisfies the fundamental QED equal-time commutation relations (24) and (25), and the Green tensor does not lead to a singular contribution to the decay rate. The Green tensor for an inhomogeneous problem of that type can always be written as a sum of the Green tensor for a homogeneous problem and some tensor that obeys a source-free wave equation and ensures the boundary conditions to be satisfied [22]. Since the guest atom is situated in an empty cavity, the relevant Green tensor reads as

$$G_{kk'}(\mathbf{r}, \mathbf{r}_A, \omega_A) = G_{kk'}^{\text{V}}(\mathbf{r}, \mathbf{r}_A, \omega_A) + \tilde{G}_{kk'}(\mathbf{r}, \mathbf{r}_A, \omega_A) \quad (\mathbf{r} \rightarrow \mathbf{r}_A) \quad (53)$$

where  $G_{kk'}^{\text{V}}(\mathbf{r}, \mathbf{r}_A, \omega_A)$  is simply the vacuum Green tensor, which is given by Eqs. (B1) – (B3) with  $\epsilon(\omega) = 1$ , and  $\tilde{G}_{kk'}(\mathbf{r}, \mathbf{r}_A, \omega_A)$  describes the effect of reflection at the cavity surface. Obviously,  $G_{kk'}^{\text{V}}(\mathbf{r}, \mathbf{r}_A, \omega_A)$  has no longitudinal imaginary part,

$$\text{Im } G_{kk'}^{\text{V}\parallel}(\mathbf{r}, \mathbf{r}_A, \omega_A) = 0 \quad (\mathbf{r} \rightarrow \mathbf{r}_A) \quad (54)$$

Since the tensor  $\tilde{G}_{kk'}(\mathbf{r}, \mathbf{r}_A, \omega_A)$  is related to a source-free problem, it is transverse, and hence

$$\tilde{G}_{kk'}^{\parallel}(\mathbf{r}, \mathbf{r}_A, \omega_A) = 0 \quad (\mathbf{r} \rightarrow \mathbf{r}_A). \quad (55)$$

The imaginary part of  $G_{kk'}(\mathbf{r}_A, \mathbf{r}_A, \omega_A)$  is therefore equal to the imaginary part of the transverse part of the Green tensor, so that the rate formula (37) in the real cavity model reads

$$\Gamma_{\text{GL}} = \frac{2\omega_A^2 \mu_k \mu_{k'}}{\hbar \epsilon_0 c^2} \text{Im} G_{kk'}^{\perp}(\mathbf{r}_A, \mathbf{r}_A, \omega_A). \quad (56)$$

In other words, in the real cavity model the longitudinal field does not contribute to the decay rate. Thus, the longitudinal decay rate  $\Gamma_{\text{GL}}^{\parallel}$  given in [10] is an artifact.

In order to calculate  $\Gamma_{\text{GL}}$  further, let us again consider a spherical cavity of radius  $R$  in bulk material, with the guest atom being situated at the center of the sphere. The Green tensor for a spherical two-layer system is given in Appendix C. From Eqs. (53) – (55) together with Eq. (B5) [for  $\epsilon(\omega) = 1$ ] and Eq. (C22) it follows that

$$\text{Im} G_{kk'}^{\perp}(\mathbf{r}_A, \mathbf{r}_A, \omega_A) = \frac{\omega_A}{6\pi c} \left[ 1 + \text{Re} C_1^N(\omega_A) \right] \delta_{kk'}, \quad (57)$$

with the reflection coefficient  $C_1^N(\omega_A)$  being given by Eq. (C23). Hence, for a spherical cavity the spontaneous decay rate (56) takes the form of

$$\Gamma_{\text{GL}} = \Gamma_0 \left[ 1 + \text{Re} C_1^N(\omega_A) \right], \quad (58)$$

where  $\Gamma_0$  is the free-space spontaneous emission rate (1). The reflection coefficient  $C_1^N(\omega_A)$  in Eq. (58) is a function of  $R$  and given in Eq. (C23) explicitly. For  $\omega_A R/c = 2\pi R/\lambda_A \ll 1$  we expand it in powers of  $R$  to obtain

$$C_1^N(\omega_A) = -\frac{3i[\epsilon(\omega_A)-1]}{2\epsilon(\omega_A)+1} \left( \frac{c}{\omega_A R} \right)^3 - \frac{9i[4\epsilon^2(\omega_A)-3\epsilon(\omega_A)-1]}{5[2\epsilon(\omega_A)+1]^2} \left( \frac{c}{\omega_A R} \right) + \frac{9\epsilon^{5/2}(\omega_A)}{[2\epsilon(\omega_A)+1]^2} - 1 + \mathcal{O}(R), \quad (59)$$

from which it follows that

$$\begin{aligned} \Gamma_{\text{GL}} = \Gamma_0 \left\{ \frac{9\epsilon_I(\omega_A)}{|2\epsilon(\omega_A)+1|^2} \left( \frac{c}{\omega_A R} \right)^3 + \frac{9\epsilon_I(\omega_A)[28|\epsilon(\omega_A)|^2+12\epsilon_R(\omega_A)+1]}{5|2\epsilon(\omega_A)+1|^4} \left( \frac{c}{\omega_A R} \right) \right. \\ \left. + \frac{9\eta(\omega_A)}{|2\epsilon(\omega_A)+1|^4} [4|\epsilon(\omega_A)|^4 + 4\epsilon_R(\omega_A)|\epsilon(\omega_A)|^2 + \epsilon_R^2(\omega_A) - \epsilon_I^2(\omega_A)] \right. \\ \left. - \frac{9\kappa(\omega_A)\epsilon_I(\omega_A)}{|2\epsilon(\omega_A)+1|^4} [4|\epsilon(\omega_A)|^2 + 2\epsilon_R(\omega_A)] \right\} + \mathcal{O}(R). \quad (60) \end{aligned}$$

Needless to say that when setting  $\epsilon(\omega) = 1$ , then the free-space spontaneous emission rate is recovered. When the atomic transition frequency is far from an absorption band of the medium, then absorption may be disregarded, i.e.,  $\epsilon_I(\omega_A) \approx 0$  [and hence  $\epsilon(\omega_A) \approx \epsilon_R(\omega_A)$ ,  $n(\omega_A) \approx \sqrt{\epsilon_R(\omega_A)}$ ]. From inspection of Eq. (60) we see that for  $\epsilon_I(\omega_A) \rightarrow 0$  the term proportional to  $R^0$  is the leading term, which exactly gives rise to the rate formula (3) together with the correction factor (5), i.e., we recover the familiar result derived in [6] for real refractive index. We further see that for an absorbing medium the rate formula cannot be given in the form of Eq. (7) together with Eq. (8), as is suggested in [10]. Equation (60) reveals that for an absorbing medium terms proportional to  $R^{-3}$  and  $R^{-1}$  are observed, so that the decay rate sensitively depends on the radius of the sphere. In particular, the near-field term proportional to  $R^{-3}$  can again be regarded as corresponding to nonradiative decay via dipole-dipole energy transfer from the guest atom to the medium.

It should be pointed out that the condition that  $\omega_A R/c \ll 1$ ; i.e., the (optical) wavelength  $\lambda_A$  of the atomic transition must be large compared with the radius  $R$  of the cavity, is in full agreement with the Markov approximation used in order to introduce a decay rate. From inspection of Eq. (C23) it is seen that the (real part of the) reflection coefficient  $C_1^N(\omega)$  becomes a rapidly varying function of frequency for  $\omega R/c \gtrsim 1$ , and hence the Markov approximation fails. In that case the sphere acts like a micro-cavity resonator and memory effects must be included in the temporal evolution of the atom, which prevents the excited state from decaying exponentially.

## V. DISCUSSION

To illustrate the results, we have computed the (virtual cavity model) decay rate  $\Gamma_{\text{CM}}$ , Eq. (50) – (52), and the (real cavity model) decay rate  $\Gamma_{\text{GL}}$ , Eq. (60), of an atom in a spherical cavity of radius  $R$  in a surrounding medium with the single-resonance model permittivity

$$\epsilon(\omega) = 1 + \frac{\omega_P^2}{\omega_T^2 - \omega^2 - i\gamma\omega_T}. \quad (61)$$

Plots of the rates as functions of the atomic transition frequency are given in Figs. 1 – 6. The figures reveal that the two models can yield decay rates that are quite different from each other. Far from the absorption band of the medium the difference is rather quantitative than qualitative [Figs. 2 and 4]. In the absorption band and in the vicinity of the absorption band, i.e., in the region between the medium resonance  $\omega_T$  and the longitudinal frequency  $\omega_L = \sqrt{\omega_T^2 + \omega_P^2}$  (in the figures,  $\omega_L = 1.1\omega_T$ ), a quantitatively and qualitatively different behavior of the two rates can be observed [Figs. 1, 3, 5, and 6]. In particular, the rate obtained with the real cavity model can substantially exceed the rate obtained with the virtual cavity model. The differences between the two rates are less pronounced for strong absorption; i.e., when the value of the bandwidth parameter  $\gamma$  in Eq. (61) is sufficiently large (compare Fig. 1 with Fig. 3, and Fig. 5 with Fig. 6). In that region the rates sensitively respond to a change of the radius of the cavity (compare Fig. 1 with Fig. 5, and Fig. 3 with Fig. 6).

Obviously, an excited atom in an absorbing medium undergoes both radiative and non-radiative damping, and in dense media nonradiative decay can be much faster than radiative one. In particular, for small cavity radius the  $\sim R^{-3}$  dipole-dipole energy transfer terms in the two rates can strongly enhance them. Since the radiationless decay typically happens at the longitudinal frequency  $\omega_L$ , one observes, for sufficiently small values of  $\gamma$ , a shift of the maximum of the decay rate from  $\omega_T$  to  $\omega_L$  with decreasing value of  $R$  (compare Fig. 5 with Fig. 1). Even when the atomic transition frequency is relatively far from the medium resonance, so that the imaginary part of the permittivity becomes relatively small, the values of the two rates can notably differ from those obtained from Eq. (3) together with either Eq. (4) or (5), because of the  $\sim R^{-3}$  near field contributions to the rates. It should be stressed that Eqs. (3) – (5) apply only when nonradiative decay can be fully excluded from consideration. Otherwise the near-field terms can give rise to observable effects, as is illustrated in Figs. 2 and 4.

The rates  $\Gamma_{\text{CM}}$  and  $\Gamma_{\text{GL}}$  differ essentially in the way the cavity radius is introduced. As already mentioned, in the virtual cavity model the needed coincidence limit of the two

spatial arguments of the imaginary part of the Green tensor cannot be performed, because of the singularity of the Green tensor of the (undisturbed) medium, and regularization is required. In the paper, a small fictitious distance  $|\mathbf{r} - \mathbf{r}'| \neq 0$  between two neighboring atomic positions inside a sphere of radius  $R$  is kept in order to get a finite value, and the result is then averaged with regard to  $\mathbf{r}$  and  $\mathbf{r}'$  separately over the sphere. In contrast, in the real cavity model the limit  $\mathbf{r}, \mathbf{r}' \rightarrow \mathbf{r}_A$  can be performed exactly and a proper rate can be obtained,  $R$  being the radius of the real cavity. From the above it is suggested that the value of the parameter  $R$  may be different in the two models in order to fit each other (note that in Figs. 1 – 6 the two rates are compared for equal values of  $R$ ).

Another consequence of the via smoothing introduced radius of the sphere in the virtual cavity model is that there is a non-vanishing  $\sim R^{-3}$  longitudinal-field contribution to the decay rate. Hence, the nonradiative dipole-dipole energy transfer from the atom to the surrounding medium is obtained from the interaction of both transverse and longitudinal electromagnetic field components with the atom,  $\Gamma_{\text{CM}} = \Gamma_{\text{CM}}^{\parallel} + \Gamma_{\text{CM}}^{\perp}$ . On the contrary, the real cavity model leads to a decay rate that solely results from the interaction of the atom with the transverse field,  $\Gamma_{\text{GL}} = \Gamma_{\text{GL}}^{\perp}$ . Here, the dipole-dipole energy transfer fully corresponds to a second-order process via virtual photons. It is worth noting that for not too small values of the radius of the virtual cavity (in our example,  $R \gtrsim 0.1 \lambda_A$ ) the contribution of  $\Gamma_{\text{CM}}^{\parallel}$  to  $\Gamma_{\text{CM}}$  is small, so that it may be disregarded and hence  $\Gamma_{\text{CM}} \approx \Gamma_{\text{CM}}^{\perp}$  (see Figs. 5 and 6).

Equation (37) defines the total energy relaxation rate of the (two-level) atom, which results from both radiative and nonradiative decay, and the question arises of what is the spontaneous emission rate. In [10] the transverse contribution to the decay rate is associated with spontaneous emission, whereas the longitudinal contribution is associated with nonradiative decay. However, the exact result obtained with the real cavity model reveals that there is no longitudinal contribution to the decay rate, and hence the transverse contribution must be associated with both spontaneous emission and nonradiative decay. Similarly, the decay rate obtained from the study of the resonant energy transfer between two guest molecules

surrounded by a perfect lattice of absorbing molecules contains only transverse-field contributions and describes both radiative and nonradiative relaxation processes [11,12]. In [12] it is suggested that the spontaneous emission rate be identified with the  $R$ -independent (far-field) contribution to the decay rate. Since the  $\sim R^{-3}$  near field contribution may be regarded as resulting from nonradiative decay via dipole-dipole energy transfer, the question remains of what is the meaning of the remaining terms. Moreover, from our analysis of, e.g., the real cavity model it is seen that  $R$  must not substantially exceed the atomic transition wavelength  $\lambda_A$ . Otherwise, the Markov approximation does not apply and the calculated decay rate becomes unphysical. In order to answer the question of what is really spontaneous emission, the model should be extended such that light detection at certain distances from the guest atom is included.

Both in the virtual cavity model and the real cavity model the dielectric is described in terms of a continuous polarization field that does not resolve the positions of the microscopic constituents of the medium. In reality an excited guest atom does of course not interact with a continuous medium, but it “sees” the discrete distribution of the microscopic constituents of the medium, at least the nearest-neighbor grouping. Hence a refined treatment of the medium should also allow for the presence in the cavity of nearest-neighboring medium species whose interaction with the guest atom is considered separately. The enlarged cavity can then be chosen such that the guest atom cannot “resolve” the discrete structure of the medium outside the cavity and the continuous description applies [23,24].

## ACKNOWLEDGMENTS

The authors thank M. Fleischhauer for helpful comments. S. S. likes to thank J. Audretsch, F. Burgbacher, and K. Krutitsky for helpful discussions during his stay at the University of Konstanz.

## APPENDIX A: MARKOV APPROXIMATION

Equation (32) can be formally integrated to obtain

$$\hat{f}_i(\mathbf{r}, \omega, t) = \hat{f}_{\text{free } i}(\mathbf{r}, \omega, t) + \frac{\omega_{21}\omega}{c^2} \sqrt{\frac{\epsilon_I(\mathbf{r}, \omega)}{\hbar\pi\epsilon_0}} (d_{21})_k G_{ki}^*(\mathbf{r}_A, \mathbf{r}, \omega) \int_{t'}^t d\tau e^{-i\omega(t-\tau)} \hat{A}_{12}(\tau), \quad (\text{A1})$$

where  $\hat{\mathbf{f}}_{\text{free}}(\mathbf{r}, \omega, t)$  evolves freely. Substituting in the vector potential in Eqs. (29) – (31) for  $\hat{f}_i(\mathbf{r}, \omega, t)$  the expression given in Eq. (A1) yields a system of integro-differential equations for the atomic quantities, which cannot be solved analytically in general. Usually the Markov approximation is introduced. It is assumed that (after performing the  $\omega$  integration) the time integral effectively runs over a small correlation time interval  $\tau_c$ . As long as we require that  $t - t' \gg \tau_c$ , we may extend the lower limit of the  $\tau$  integral in Eq. (A1) to minus infinity with little error. Further we require that  $\tau_c$  be small on a time scale on which the atomic system is changed owing to the coupling to the electromagnetic field. In this case in the  $\tau$  integral in Eq. (A1) the slowly varying atomic quantity  $\hat{A}_{12}(\tau)e^{i\omega_{21}\tau}$  can be taken at time  $t$  and put in front of the integral,

$$\begin{aligned} \int_{t'}^t d\tau e^{-i\omega(t-\tau)} \hat{A}_{12}(\tau) &\approx \int_{-\infty}^t d\tau e^{-i\omega(t-\tau)} \hat{A}_{12}(\tau) \\ &\approx \hat{A}_{12}(t) \int_{-\infty}^t d\tau e^{-i(\omega-\omega_{21})(t-\tau)} = \hat{A}_{12}(t) \zeta(\omega_{21} - \omega) \end{aligned} \quad (\text{A2})$$

$[\zeta(x) = \pi\delta(x) + i\mathcal{P}x^{-1}$ ;  $\mathcal{P}$  denotes the principal value]. Thus, the future of the system is now determined by the present time only. We substitute in Eq. (A1) for the time integral the expression given in Eq. (A2), calculate the vector potential, Eqs. (26) and (27). With the help of the relation (see, e.g., [18])

$$\int d^3\mathbf{s} \frac{\omega^2}{c^2} \epsilon_I(\mathbf{s}, \omega) G_{km}(\mathbf{r}, \mathbf{s}, \omega) G_{lm}^*(\mathbf{r}', \mathbf{s}, \omega) = \text{Im} G_{kl}(\mathbf{r}, \mathbf{r}', \omega) \quad (\text{A3})$$

we find after some calculation

$$\hat{A}_i^{(+)}(\mathbf{r}_A, t) = \hat{A}_{\text{free } i}^{(+)}(\mathbf{r}_A, t) + \frac{\omega_{21}}{\pi\epsilon_0 c^2} (d_{21})_k \int_0^\infty d\omega \zeta(\omega_{21} - \omega) \text{Im} G_{ik}(\mathbf{r}_A, \mathbf{r}_A, \omega) \hat{A}_{12}(t). \quad (\text{A4})$$

In order to obtain Eqs. (34) – (36), we eventually substitute in Eqs. (29) – (31) for the positive and negative frequency parts of the vector potential the expressions according to Eq. (A4). It can be easily seen that the real part of the  $\zeta$  function (i.e., the  $\delta$  function) in Eq. (A4) leads to  $\Gamma$  given in Eq. (37). The principal-value integral in Eq. (A4) which arises from the imaginary part of the  $\zeta$  function contributes to the Lamb shift and reads

$$\delta\omega = \frac{2\omega_{21}^2 (d_{21})_k (d_{21})_{k'}}{\hbar\epsilon_0 c^2 \pi} \int_0^\infty d\omega \frac{\text{Im} G_{kk'}(\mathbf{r}_A, \mathbf{r}_A, \omega)}{\omega - \omega_{21}}, \quad (\text{A5})$$

which can be rewritten as

$$\delta\omega = \frac{2\omega_{21}^2 (d_{21})_k (d_{21})_{k'}}{\hbar\epsilon_0 c^2} \left[ \text{Re} G_{kk'}(\mathbf{r}_A, \mathbf{r}_A, \omega_{21}) - \frac{1}{\pi} \int_0^\infty d\omega \frac{\text{Im} G_{ik}(\mathbf{r}_A, \mathbf{r}_A, \omega)}{\omega + \omega_{21}} \right]. \quad (\text{A6})$$

Equation (A6) holds because of the Kramers-Kronig relation (or Titchmarsh's theorem) for the Green function. Note that the real part of the vacuum Green function is infinite for  $\mathbf{r} = \mathbf{r}' = \mathbf{r}_A$  and regularization is required. The resulting vacuum Lamb shift may be thought of as being included in the atomic transition frequency, so that  $\delta\omega$  in Eq. (36) may be regarded as being solely due to the surrounding dielectric.

## APPENDIX B: GREEN TENSOR FOR A HOMOGENEOUS DIELECTRIC

Following [10,19], the Green tensor for bulk material can be given by

$$G_{kk'}(\mathbf{r}, \mathbf{r}', \omega) = G_{kk'}^\parallel(\mathbf{r}, \mathbf{r}', \omega) + G_{kk'}^\perp(\mathbf{r}, \mathbf{r}', \omega), \quad (\text{B1})$$

where ( $\boldsymbol{\rho} = \mathbf{r} - \mathbf{r}'$ )

$$G_{kk'}^\parallel(\mathbf{r}, \mathbf{r}', \omega) = -\frac{c^2}{4\pi\omega^2\epsilon(\omega)} \left[ \frac{4\pi}{3} \delta(\boldsymbol{\rho}) \delta_{kk'} + \left( \delta_{kk'} - \frac{3\rho_k \rho_{k'}}{\rho^2} \right) \frac{1}{\rho^3} \right] \quad (\text{B2})$$

and

$$G_{kk'}^\perp(\mathbf{r}, \mathbf{r}', \omega) = \frac{c^2}{4\pi\omega^2\epsilon(\omega)} \left\{ \left( \delta_{kk'} - \frac{3\rho_k \rho_{k'}}{\rho^2} \right) \frac{1}{\rho^3} + k^3 \left[ \left( \frac{1}{k\rho} + \frac{i}{(k\rho)^2} - \frac{1}{(k\rho)^3} \right) \delta_{kk'} - \left( \frac{1}{k\rho} + \frac{3i}{(k\rho)^2} - \frac{3}{(k\rho)^3} \right) \frac{\rho_k \rho_{k'}}{\rho^2} \right] e^{ik\rho} \right\}, \quad (\text{B3})$$

are related to the longitudinal and transverse electric fields. In Eq. (B3), the complex wave number

$$k = \sqrt{\epsilon(\omega)} \frac{\omega}{c} = [\eta(\omega) + i\kappa(\omega)] \frac{\omega}{c} \quad (\text{B4})$$

has been introduced. In particular for small values of  $|k\rho|$ ,  $|k\rho| \ll 1$ , the exponential  $e^{ik\rho}$  in Eq. (B3) can be expanded to obtain

$$G_{kk'}^\perp(\mathbf{r}, \mathbf{r}', \omega) = \frac{1}{4\pi} \left\{ \frac{\rho_k \rho_{k'}}{2\rho^3} + \frac{\delta_{kk'}}{2\rho} + \frac{2i\omega}{3c} [\eta(\omega) + i\kappa(\omega)] \delta_{kk'} \right\} + \mathcal{O}(\rho). \quad (\text{B5})$$

### APPENDIX C: GREEN TENSOR FOR AN EMPTY SPHERE SURROUNDED BY A HOMOGENEOUS DIELECTRIC

Following [25], the Green tensor of a system that consists of an empty sphere surrounded by a homogeneous dielectric can be given in terms of spherical Bessel functions and spherical harmonics. When  $\mathbf{r}$  and  $\mathbf{r}'$  lie in the sphere (with the center of the sphere being the origin of the coordinate system), then the associated Green tensor  $\mathbf{G}(\mathbf{r}, \mathbf{r}', \omega)$  is given by

$$\mathbf{G}(\mathbf{r}, \mathbf{r}', \omega) = \mathbf{G}^V(\mathbf{r}, \mathbf{r}', \omega) + \tilde{\mathbf{G}}(\mathbf{r}, \mathbf{r}', \omega), \quad (\text{C1})$$

where  $\mathbf{G}^V(\mathbf{r}, \mathbf{r}', \omega)$  is the vacuum Green tensor, and

$$\begin{aligned} \tilde{\mathbf{G}}(\mathbf{r}, \mathbf{r}', \omega) = & \frac{i\omega}{4\pi c} \sum_{e,o} \sum_{n=1}^{\infty} \sum_{m=0}^n \left\{ \frac{2n+1}{n(n+1)} \frac{(n-m)!}{(n+m)!} \right. \\ & \left. \times (2 - \delta_{0m}) \left[ C_n^M(\omega) \mathbf{M}_{e, nm} \left( \mathbf{r}, \frac{\omega}{c} \right) \mathbf{M}_{e, nm} \left( \mathbf{r}', \frac{\omega}{c} \right) + C_n^N(\omega) \mathbf{N}_{e, nm} \left( \mathbf{r}, \frac{\omega}{c} \right) \mathbf{N}_{e, nm} \left( \mathbf{r}', \frac{\omega}{c} \right) \right] \right\}. \end{aligned} \quad (\text{C2})$$

Here  $\mathbf{M}_{e, nm}(\mathbf{r}, k)$  and  $\mathbf{N}_{e, nm}(\mathbf{r}, k)$  are the (even and odd) vector Debye potentials, and the quantities  $C_n^{M,N}(\omega)$  are the generalized reflection coefficients. Introducing the abbreviating notations

$$J_{ni} = j_n(k_i R), \quad (\text{C3})$$

$$H_{ni} = h_n^{(1)}(k_i R), \quad (\text{C4})$$

$$J'_{ni} = \frac{1}{\rho} \left. \frac{d[\rho j_n(\rho)]}{d\rho} \right|_{\rho=k_i R}, \quad (\text{C5})$$

$$H'_{ni} = \frac{1}{\rho} \left. \frac{d[\rho h_n^{(1)}(\rho)]}{d\rho} \right|_{\rho=k_i R} \quad (\text{C6})$$

( $k_1 = \sqrt{\epsilon(\omega)}\omega/c$ ,  $k_2 = \omega/c$ ), the reflection coefficients can be given by

$$C_n^{M,N}(\omega) = \frac{T_{F,n}^{H,V}(\omega) R_{P,n}^{H,V}(\omega)}{T_{P,n}^{H,V}(\omega)}, \quad (\text{C7})$$

where

$$R_{P,n}^H(\omega) = \frac{k_2 H'_{n2} H_{n1} - k_1 H'_{n1} H_{n2}}{k_2 J_{n1} H'_{n2} - k_1 J'_{n1} H_{n2}}, \quad (\text{C8})$$

$$R_{P,n}^V(\omega) = \frac{k_2 H_{n2} H'_{n1} - k_1 H_{n1} H'_{n2}}{k_2 J'_{n1} H_{n2} - k_1 J_{n1} H'_{n2}}, \quad (\text{C9})$$

$$T_{P,n}^H(\omega) = \frac{k_2 [J_{n2} H'_{n2} - J'_{n2} H_{n2}]}{k_2 J_{n1} H'_{n2} - k_1 J'_{n1} H_{n2}}, \quad (\text{C10})$$

$$T_{F,n(\omega)}^H = \frac{k_2 [J'_{n2} H_{n2} - J_{n2} H'_{n2}]}{k_2 J'_{n2} H_{n1} - k_1 J_{n2} H'_{n1}}, \quad (\text{C11})$$

$$T_{P,n}^V(\omega) = \frac{k_2 [J'_{n2} H_{n2} - J_{n2} H'_{n2}]}{k_2 J'_{n1} H_{n2} - k_1 J_{n1} H'_{n2}}, \quad (\text{C12})$$

$$T_{F,n}^H(\omega) = \frac{k_2 [J_{n2} H'_{n2} - J'_{n2} H_{n2}]}{k_2 J_{n2} H'_{n1} - k_1 J'_{n2} H_{n1}}. \quad (\text{C13})$$

The vector Debye potentials are defined by

$$\mathbf{M}_{\circ nm}(\mathbf{r}, k) = \nabla \times [\psi_{\circ nm}(\mathbf{r}, k) \mathbf{r}], \quad (\text{C14})$$

$$\mathbf{N}_{\circ nm}(\mathbf{r}, k) = \frac{1}{k} \nabla \times \nabla \times [\psi_{\circ nm}(\mathbf{r}, k) \mathbf{r}] \quad (\text{C15})$$

with

$$\psi_{\circ nm}(\mathbf{r}, k) = j_n(kr) P_n^m(\cos \theta) \begin{pmatrix} \cos \\ \sin \end{pmatrix} m\phi, \quad (\text{C16})$$

and can be given by

$$\mathbf{M}_{\circ nm}(\mathbf{r}, k) = \frac{im}{\sin \theta} j_n(kr) P_n^m(\cos \theta) \begin{pmatrix} \cos \\ \sin \end{pmatrix} m\phi \mathbf{e}_\theta - j_n(kr) \frac{dP_n^m(\cos \theta)}{d\theta} \begin{pmatrix} \cos \\ \sin \end{pmatrix} m\phi \mathbf{e}_\phi, \quad (\text{C17})$$

$$\begin{aligned} \mathbf{N}_{\circ nm}(\mathbf{r}, k) &= \frac{n(n+1)}{kr} j_n(kr) P_n^m(\cos \theta) \begin{pmatrix} \cos \\ \sin \end{pmatrix} m\phi \mathbf{e}_r \\ &+ \frac{1}{kr} \frac{d[rj_n(kr)]}{dr} \left[ \frac{dP_n^m(\cos \theta)}{d\theta} \begin{pmatrix} \cos \\ \sin \end{pmatrix} m\phi \mathbf{e}_\theta \mp \frac{im}{\sin \theta} P_n^m(\cos \theta) \begin{pmatrix} \sin \\ \cos \end{pmatrix} m\phi \mathbf{e}_\phi \right], \end{aligned} \quad (\text{C18})$$

$j_n(kr)$  is the spherical Bessel function of the first kind and  $P_n^m(\cos\theta)$  is the associated Legendre polynomial. Note that from Eqs. (C14) and (C15) it follows that  $\mathbf{G}(\mathbf{r}, \mathbf{r}', \omega)$  is a (two-sided) transverse tensor function.

Since for  $kr \rightarrow 0$  we have

$$j_n(kr) \xrightarrow{kr \rightarrow 0} \frac{(kr)^n}{(2n+1)!!} \left( 1 - \frac{1}{2(2n+3)} + \dots \right), \quad (\text{C19})$$

from inspection of Eqs. (C17) and (C18) we find that

$$\mathbf{M}_{\circ nm}(\mathbf{r}, k) \xrightarrow{kr \rightarrow 0} (kr)^n, \quad (\text{C20})$$

$$\mathbf{N}_{\circ nm}(\mathbf{r}, k) \xrightarrow{kr \rightarrow 0} (kr)^{n-1}. \quad (\text{C21})$$

Hence, at the center of the sphere only the TM-wave vector Debye potentials  $\mathbf{N}_{\circ 10}(\mathbf{r}, k)$  and  $\mathbf{N}_{\circ 11}(\mathbf{r}, k)$  contribute to  $\tilde{\mathbf{G}}(\mathbf{r}, \mathbf{r}', \omega)$  in Eq. (C2),

$$\tilde{G}_{kk'}(\mathbf{r}, \mathbf{r}', \omega) \Big|_{\mathbf{r}=\mathbf{r}'=0} = \frac{i\omega}{6\pi c} C_1^N(\omega) \delta_{kk'}, \quad (\text{C22})$$

where  $[n \equiv \sqrt{\epsilon(\omega)}]$

$$C_1^N(\omega) = \frac{[i + z(n+1) - iz^2n - z^3n^2/(n+1)] e^{iz}}{\sin z - z(\cos z + in \sin z) + iz^2n \cos z - z^3(\cos z - in \sin z)n^2/(n^2-1)} \quad (\text{C23})$$

with

$$z = \frac{R\omega}{c}. \quad (\text{C24})$$

## REFERENCES

- [1] A. Einstein, *Z. Physik* **18**, 121 (1917).
- [2] P.W. Milonni, *The Quantum Vacuum: An Introduction to Quantum Electrodynamics*, (Academic, San Diego, 1994).
- [3] G. Nienhuis and C.Th.J. Alkemade, *Physica* **81C**, 181 (1976).
- [4] for a review on local fields, see O. Keller, in: *Progress in Optics*, Vol. XXXVII, ed. E. Wolf (North-Holland, Amsterdam, 1997) p. 257.
- [5] J. Knoester and S. Mukamel, *Phys. Rev. A* **40**, 7065 (1989).
- [6] R.J. Glauber and M. Lewenstein, *Phys. Rev. A* **43**, 467 (1991).
- [7] G.L.J.A. Rikken and Y.A.R.R. Kessener, *Phys. Rev. Lett.* **74**, 880 (1995).
- [8] F.J.P. Schuurmans, D.T.N. de Lang, G.H. Wegdam, R. Sprik, and A. Lagendijk, *Phys. Rev. Lett.* **80**, 5077 (1998).
- [9] S.M. Barnett, B. Huttner, and R. Loudon, *Phys. Rev. Lett.* **68**, 3698 (1992).
- [10] S.M. Barnett, B. Huttner, R. Loudon, and R. Matloob, *J. Phys. B: At. Mol. Opt. Phys.* **29**, 3763 (1996).
- [11] G. Juzeliūnas and D.L. Andrews, *Phys. Rev. B* **49**, 8751 (1994).
- [12] G. Juzeliūnas, *Phys. Rev. A* **55**, R4015 (1997).
- [13] S. Scheel, L. Knöll, D.-G. Welsch, and S.M. Barnett, submitted to *Phys. Rev. A*, e-print *quant-ph/9811067*.
- [14] M. Fleischhauer, e-print *quant-ph/9902076*.
- [15] P.D. Craig and T. Thirunamachandran, *Molecular Quantum Electrodynamics*, (Academic, London, 1984).

- [16] T. Gruner and D.-G. Welsch, Phys. Rev. A **53**, 1818 (1996).
- [17] Ho Trung Dung, L. Knöll, and D.-G. Welsch, Phys. Rev. A **57**, 3931 (1998).
- [18] S. Scheel, L. Knöll, and D.-G. Welsch, Phys. Rev. A **58**, 700 (1998).
- [19] A.A. Abrikosov, L.P. Gorkov, and I.E. Dzyaloshinski, *Methods of Quantum Field Theory in Statistical Physics*, (Dover Publications, New York, 1975).
- [20] M. Born and E. Wolf, *Principles of Optics*, (Pergamon, Oxford, 1993).
- [21] Note that in [13] the average is taken with respect to the distance  $\mathbf{r} - \mathbf{r}_A$ , which leads to somewhat different regularization factors.
- [22] W.C. Chew, *Waves and Fields in Inhomogeneous Media*, (IEEE Press, New York, 1995).
- [23] K.V. Krutitsky and S.V. Suhov, J. Phys. B: At. Mol. Opt. Phys. **30**, 5341 (1997).
- [24] K.V. Krutitsky and J. Audretsch, J. Phys. B: At. Mol. Opt. Phys. **31**, 2633 (1998).
- [25] L.W. Li, P.S. Kooi, M.S. Leong, and T.S. Yeo, IEEE Transactions on Microwave Theory and Techniques **42**, 2302 (1994).

## FIGURES

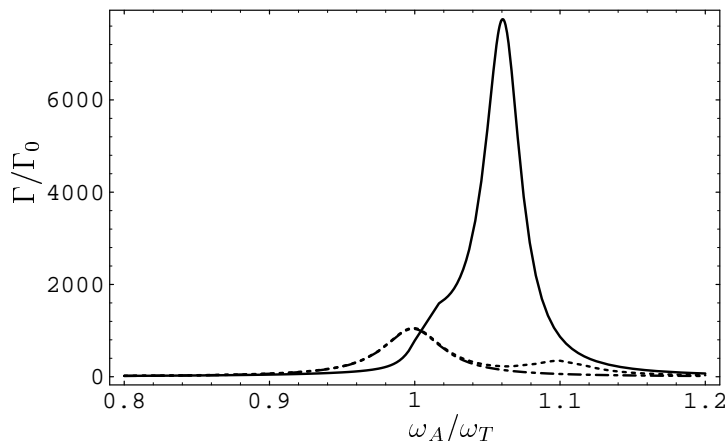


FIG. 1. The spontaneous decay rate  $\Gamma$ , Eq. (37), is shown as a function of the atomic transition frequency  $\omega_A$  near a medium resonance for the model permittivity (61) ( $\omega_P = 0.46 \omega_T$ ,  $\gamma = 0.05 \omega_T$ ) and  $R = 0.02 \lambda_A$ . The solid line corresponds to the real-cavity model,  $\Gamma_{\text{GL}}$  from Eq. (60), and the dotted line corresponds to the virtual-cavity model,  $\Gamma_{\text{CM}}$  from Eq. (50), the broken line indicating the transverse-field assisted rate  $\Gamma_{\text{CM}}^\perp$  from Eq. (52).

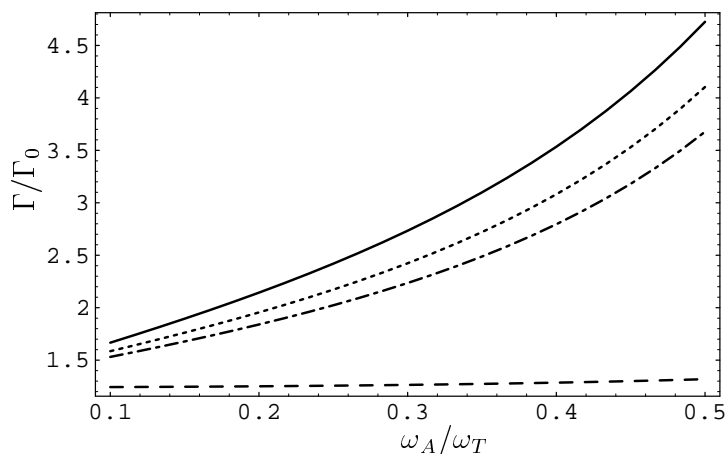


FIG. 2. The spontaneous decay rate  $\Gamma$ , Eq. (37), is shown as a function of the atomic transition frequency  $\omega_A$  far from a medium resonance for the model permittivity (61) ( $\omega_P = 0.46 \omega_T$ ,  $\gamma = 0.05 \omega_T$ ) and  $R = 0.02 \lambda_A$ . The solid line corresponds to the real-cavity model,  $\Gamma_{\text{GL}}$  from Eq. (60), and the dotted line corresponds to the virtual-cavity model,  $\Gamma_{\text{CM}}$  from Eq. (50), the broken line indicating the transverse-field assisted rate  $\Gamma_{\text{CM}}^\perp$  from Eq. (52). For comparison, the rate  $\Gamma_{\text{GL}}$  as obtained from Eq. (3) together with (5) is shown (dashed line).

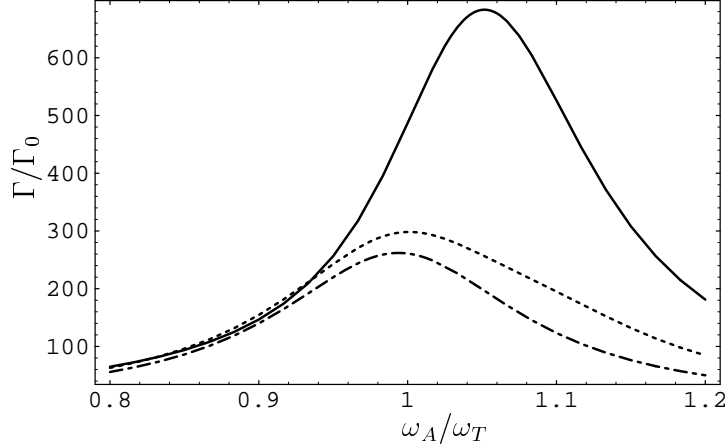


FIG. 3. The spontaneous decay rate  $\Gamma$ , Eq. (37), is shown as a function of the atomic transition frequency  $\omega_A$  near a medium resonance for the model permittivity (61) ( $\omega_P = 0.46 \omega_T$ ,  $\gamma = 0.2 \omega_T$ ) and  $R = 0.02 \lambda_A$ . The solid line corresponds to the real-cavity model,  $\Gamma_{\text{GL}}$  from Eq. (60), and the dotted line corresponds to the virtual-cavity model,  $\Gamma_{\text{CM}}$  from Eq. (50), the broken line indicating the transverse-field assisted rate  $\Gamma_{\text{CM}}^\perp$  from Eq. (52).

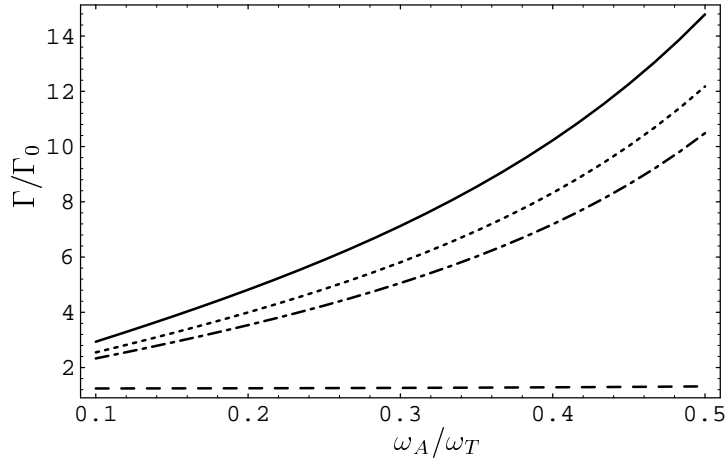


FIG. 4. The spontaneous decay rate  $\Gamma$ , Eq. (37), is shown as a function of the atomic transition frequency  $\omega_A$  far from a medium resonance for the model permittivity (61) ( $\omega_P = 0.46 \omega_T$ ,  $\gamma = 0.2 \omega_T$ ) and  $R = 0.02 \lambda_A$ . The solid line corresponds to the real-cavity model,  $\Gamma_{\text{GL}}$  from Eq. (60), and the dotted line corresponds to the virtual-cavity model,  $\Gamma_{\text{CM}}$  from Eq. (50), the broken line indicating the transverse-field assisted rate  $\Gamma_{\text{CM}}^\perp$  from Eq. (52). For comparison, the rate  $\Gamma_{\text{GL}}$  as obtained from Eq. (3) together with (5) is shown (dashed line).

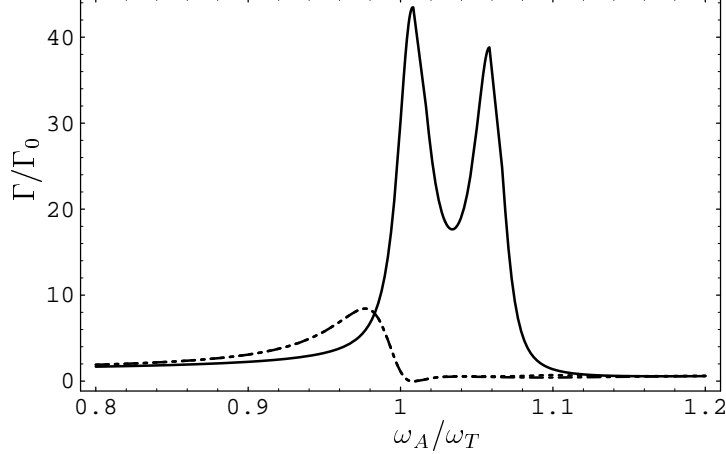


FIG. 5. The spontaneous decay rate  $\Gamma$ , Eq. (37), is shown as a function of the atomic transition frequency  $\omega_A$  near a medium resonance for the model permittivity (61) ( $\omega_P = 0.46 \omega_T$ ,  $\gamma = 0.05 \omega_T$ ) and  $R = 0.2 \lambda_A$ . The solid line corresponds to the real-cavity model,  $\Gamma_{\text{GL}}$  from Eq. (60), and the dotted line corresponds to the virtual-cavity model,  $\Gamma_{\text{CM}}$  from Eq. (50), the broken line indicating the transverse-field assisted rate  $\Gamma_{\text{CM}}^{\perp}$  from Eq. (52).

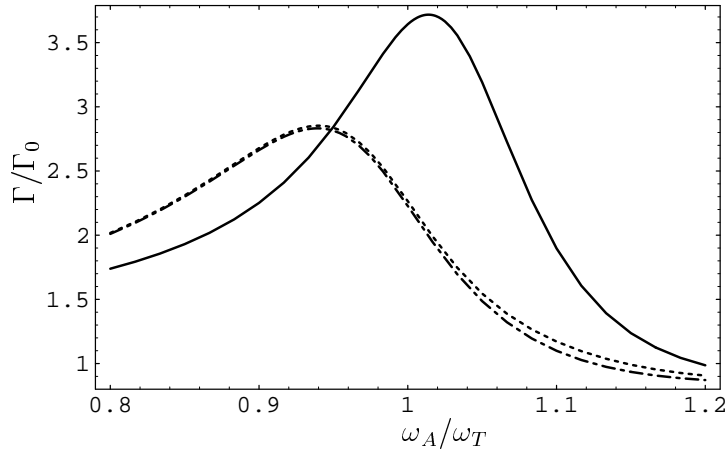


FIG. 6. The spontaneous decay rate  $\Gamma$ , Eq. (37), is shown as a function of the atomic transition frequency  $\omega_A$  near a medium resonance for the model permittivity (61) ( $\omega_P = 0.46 \omega_T$ ,  $\gamma = 0.2 \omega_T$ ) and  $R = 0.2 \lambda_A$ . The solid line corresponds to the real-cavity model,  $\Gamma_{\text{GL}}$  from Eq. (60), and the dotted line corresponds to the virtual-cavity model,  $\Gamma_{\text{CM}}$  from Eq. (50), the broken line indicating the transverse-field assisted rate  $\Gamma_{\text{CM}}^{\perp}$  from Eq. (52).